

Emissive Erbium-Doped Silicon and Germanium Oxide Nanofibers Derived from an Electrospinning Process

Ji Wu and Jeffery L. Coffler*

Department of Chemistry, Texas Christian University, Fort Worth, Texas 76129

Received August 7, 2007. Revised Manuscript Received October 4, 2007

Use of sol–gel condensation reactions with the proper precursors, in conjunction with electrospinning methods, leads to the facile formation of one-dimensional nanofibers of silicon or germanium dioxide doped with erbium. These nanowires are characterized by a combination of scanning and transmission electron microscopies, energy dispersive X-ray analysis, FT IR spectroscopy, X-ray diffraction, and photoluminescence spectroscopy. By comparing such structures with comparably sized nanofibers of erbium oxide (Er_2O_3), the influence of oxide matrix and erbium concentration on Er^{3+} luminescence in the near-infrared at 1540 nm is examined. Furthermore, an analysis of the luminescence excitation spectra of Er-doped GeO_2 nanofibers prepared by the above route with Er-doped GeO_2 NWs and Er-doped Ge NWs prepared by a different vapor–liquid–solid pathway suggests a common excitation mechanism of erbium ions in these structures assisted by GeO_x through a carrier-mediated process.

Introduction

The incorporation of optically active erbium ions into oxide matrices is a targeted component of a long-term strategy toward the fabrication of integrated optoelectronic circuits operating at $1.5 \mu\text{m}$.¹ Facile bottom-up routes to subwavelength nanofibers of this composition are of interest as they could be used as potential building blocks for waveguides and amplifiers in such a platform. Previous efforts from our laboratories have focused on the fabrication of erbium-containing silicon or germanium nanocrystals/nanowires, whereby the structure of interest could serve as the light-emitting component in this type of monolithic circuit.^{2,3} As a consequence, the second benefit imagined for one-dimensional (1-D) Er-doped group IV oxide nanofibers is to provide an alternative, well-defined experimental model analogous to oxidized Er-doped Ge and SiGe nanowires (NWs) so that the mechanism of erbium luminescence in these host materials can be further investigated in detail.

In terms of bottom-up assembly methods, sol–gel condensation reactions have been long appreciated for producing thin films of a broad range of useful oxide materials, including Er-doped group IV oxide film waveguides and

amplifiers.⁴ Recently, use of this approach in conjunction with electrospinning has been demonstrated to be an efficient technique to produce nanofibers such as TiO_2 in high yield.⁵ Therefore, a combination of sol–gel reactions using the appropriate precursors with an electrospinning technique is one appealing route to obtain erbium-doped group IV oxide nanofibers.

From a standpoint of controlling composition, one of the main advantages of this fabrication method is its use of condensed phase reactions whereby reactants can be precisely weighted such that the concentrations of erbium ions in the host materials can be easily controlled by adjusting the ratios of the erbium precursor to a given group IV oxide sol–gel precursor. Ideally, all Er^{3+} ions are left in the oxide matrices after the reaction without any loss. In addition, erbium ions can be homogeneously dispersed in the host materials without a serious erbium clustering provided that the concentrations of Er^{3+} ions are below its solubility limit in a given host material. However, in the Er-doped Ge and SiGe NWs prepared by vapor transport reactions reported previously, most of the Er^{3+} ions are concentrated on the surface of these NWs.³ Although a high-temperature postannealing can help diffuse these concentrated Er^{3+} ions into these host materials, a certain amount of Er^{3+} ions is still clustered on the surface of these NWs. Furthermore, since the load of Er^{3+} incorporation relies on a kinetic entrapment process, some of the Er^{3+} ions present in the reactor can be deposited on the inner wall of the reactor or carried away by the helium carrier gas so that the amount of erbium actually incorporated is more difficult to measure.

In terms of potential host materials for erbium ions, silica possesses multiple advantages including a broad spectral transmission range, strong tolerance to harsh chemical

* Corresponding author. E-mail: j.coffler@tcu.edu.

- (1) Kimerling, L. C. *Appl. Surf. Sci.* **2000**, 159–60, 8–13.
(2) (a) St John, J.; Coffler, J. L.; Chen, Y. D.; Pinizzotto, R. F. *J. Am. Chem. Soc.* **1999**, 121, 1888. (b) St. John, J.; Coffler, J.; Chen, Y.; Pinizzotto, R. *Appl. Phys. Lett.* **2000**, 77, 1635. (c) Senter, R. A.; Chen, Y. D.; Coffler, J. L.; Tessler, L. R. *Nano Lett.* **2001**, 1, 383. (d) St. John, J.; Coffler, J. *J. Phys. (Paris)* **2001**, 105, 7599. (e) Ji, J.; Senter, R.; Coffler, J. *Chem. Mater.* **2001**, 13, 4783. (f) Tessler, L.; Coffler, J.; Ji, J.; Senter, R. *J. Non-Cryst. Solids* **2002**, 299–302, 673. (g) Ji, J.; Senter, R.; Tessler, L. R.; Back, D.; Winter, C. H.; Coffler, J. L. *Nanotechnology* **2004**, 15, 643. (h) Senter, R. A.; Pantea, C.; Wang, Y.; Liu, H.; Zerda, T. W.; Coffler, J. L. *Phys. Rev. Lett.* **2004**, 93, 175502. (i) Samia, A.; Lou, Y.; Burda, C.; Senter, R.; Coffler, J. L. *J. Chem. Phys.* **2004**, 120, 8716.
(3) (a) Wang, Z. Y.; Coffler, J. L. *NanoLett.* **2002**, 2, 1303. (b) Wu, J.; Coffler, J. L.; Punchaipetch, P.; Wallace, R. M. *Adv. Mater.* **2004**, 16, 1444. (c) Wang, Z.; Coffler, J. L. *J. Phys. Chem. B* **2004**, 108, 2497.

- (4) Selvarajan, A.; Srinivas, T. *IEEE J. Quantum Electron.* **2001**, 37, 1117.
(5) Li, D.; Xia, Y. *Nano Lett.* **2003**, 3, 555.

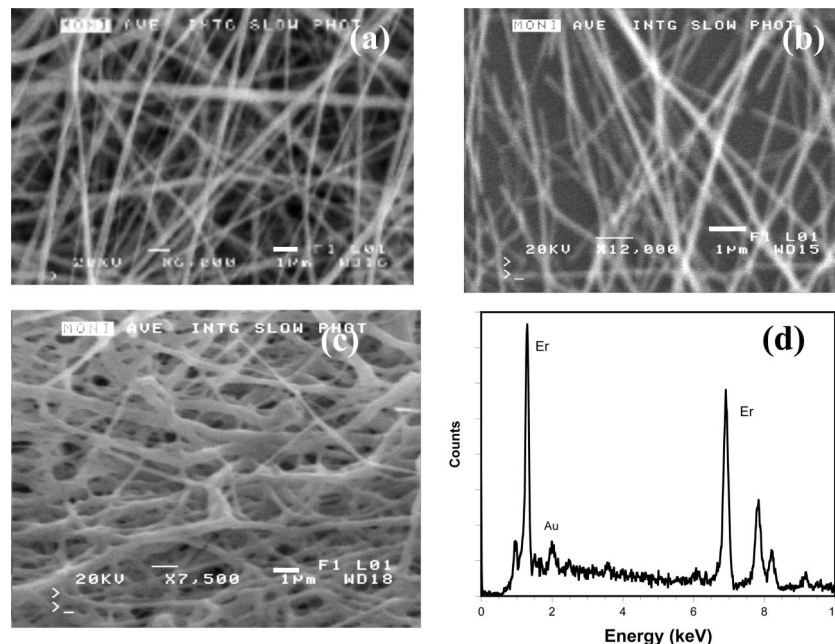


Figure 1. SEM images of (a) as-formed $\text{Er}_2\text{O}_3/\text{PVP}$ fibers, (b) the fibers annealed at $500\text{ }^\circ\text{C}$ for 3 h in air, and (c) the fibers annealed at $700\text{ }^\circ\text{C}$ for 3 h in air. (d) EDX spectrum of Er_2O_3 nanofibers. Scale bars in (a)–(c) are $1\text{ }\mu\text{m}$.

environments, high resistance to laser damage, etc.⁶ This host material is also fully compatible with the silica-based optical fiber industry and has been successfully employed to fabricate two-dimensional Er-doped film waveguides and amplifiers.⁷ Germanate-based glasses also have potential applications in optical devices because of their low transmission loss in the infrared region.⁸ These glasses also have good mechanical strength, high thermal stability, and high refractive index, which make them suitable candidates for optical fibers.⁹ Recently, optical fibers based on undoped GeO_2 glasses have been successfully used for high-power laser delivery at $2.94\text{ }\mu\text{m}$ (wavelength of an erbium-substituted yttrium aluminum garnet laser).¹⁰

In this work, Er-doped group IV oxide nanofibers of silicon and germanium with controllable erbium concentrations are fabricated successfully via an electrospinning approach that is assisted by a sol–gel process. As a control, Er_2O_3 nanofibers were also prepared in order to compare their fundamental luminescence properties with those of the other nanofibers. As-prepared nanofibers were characterized using scanning electron microscopy (SEM), energy dispersive X-ray analysis (EDX), transmission electron microscopy (TEM), and, in some cases, FT infrared (IR) vibrational spectroscopy and X-ray diffraction (XRD). The near-IR photoluminescence properties of all Er-doped nanofibers were also investigated herein. Furthermore, the PL properties of Er-doped crystalline GeO_2 nanowires prepared via a vapor–liquid–solid (VLS) synthetic route were compared

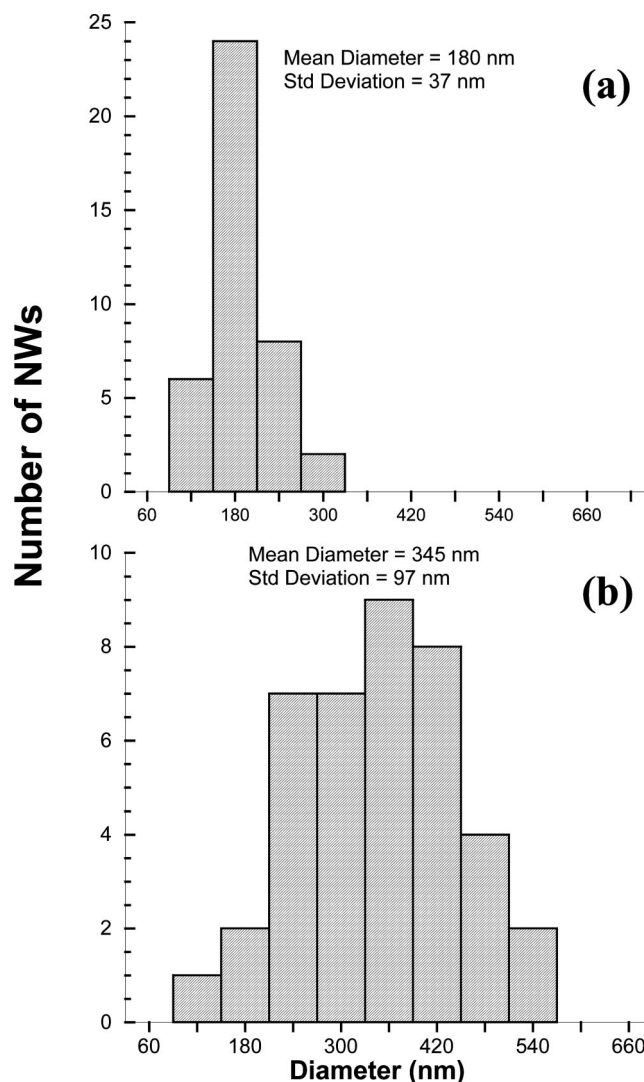


Figure 2. Diameter distributions of (a) Er_2O_3 nanofibers annealed at $500\text{ }^\circ\text{C}$ in air for 3 h and (b) as-formed $\text{Er}_2\text{O}_3/\text{PVP}$ nanofibers.

(6) Klocek, P. *Handbook of Infrared Optical Materials*; Marcel Dekker: New York, 1991.

(7) Polman, A. *J. Appl. Phys.* **1997**, *82*, 1.

(8) Pan, Z.; Morgan, S. H. *J. Lumin.* **1997**, *75*, 301.

(9) Wang, J.; Lincoln, J. R.; Brocklesby, W. S.; Deol, R. S.; Mackechnie, C. J.; Pearson, A.; Tropper, A. C.; Hanna, D. C.; Payne, D. N. *J. Appl. Phys.* **1993**, *73*, 8066.

(10) Lezal, D.; Pedlikova, J.; Kostka, P.; Bludska, J.; Poulain, M.; Zavadil, J. *J. Non-Cryst. Solids* **2001**, *284*, 288.

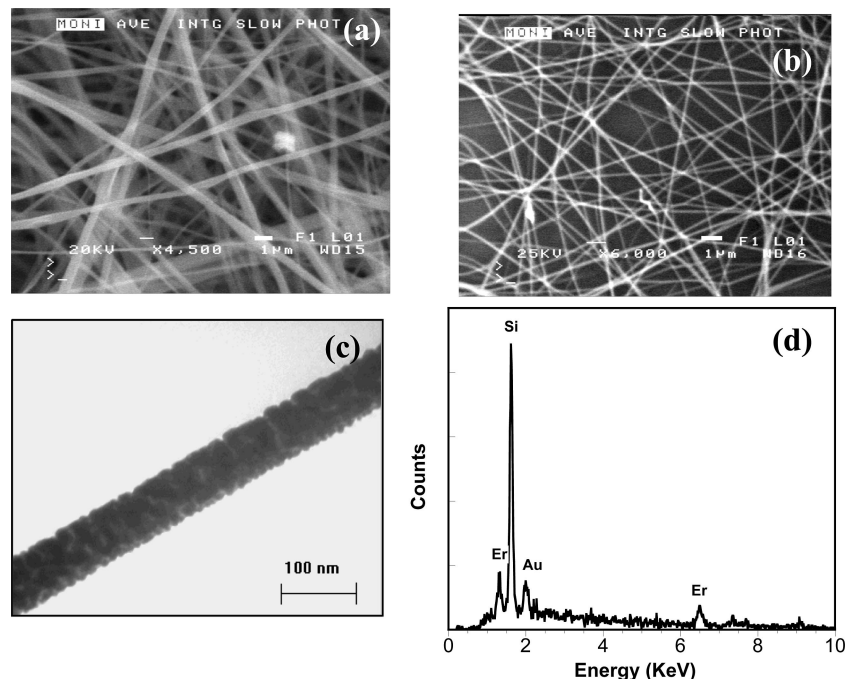


Figure 3. SEM images of (a) as-prepared Er-doped SiO₂/PVP nanofibers and (b) the nanofibers annealed at 800 °C for 3 h in air; fibers were prepared with an erbium concentration of 2%. (c) TEM image of the fibers annealed at 700 °C in air for 3 h. (d) EDX spectrum of the nanofibers confirms the presence of both Si and Er with an atomic ratio of ~50:1. Scale bars for (a) and (b) are 1 μm; (c) is 100 nm.

with analogous Er-doped GeO₂ nanofibers fabricated through the above sol-gel/electrospinning method.

Experimental Section

Fabrication of Er₂O₃ Nanofibers. Polyvinylpyrrolidone (PVP, 0.60 g, $M_w = 1.3$ M, Aldrich Chemical Co.), dissolved in 2.5 mL of absolute ethanol (AAPER Alcohol and Chemical Co.), was mixed well with 0.25 g of Er(III) isopropoxide (99.9%, Strem Chemicals) in a mixture of 1.0 mL of absolute ethanol and 1.0 mL of acetic acid (Mallinckrodt AR) by vortex shaking. PVP was selected as a templating polymer because it has good solubility in alcohols and water, which makes it compatible with the sol-gel process. The mixture was then loaded into a glass syringe equipped with a 21 gauge stainless steel needle. The needle was connected to a high-voltage direct current (dc) supply using a metal clamp. A piece of aluminum foil was used to wrap the surface of a drum that serves as a grounding electrode to collect these nanofibers. The as-formed nanofibers were exposed to air for about a week in order to completely hydrolyze the alkoxide precursors. A 25 kV accelerating voltage and a 15 cm working distance between the needle and the drum were used to carry out the electrospinning process. As-fabricated nanofibers were annealed in air at 500 °C or higher temperatures for 3 h to remove the PVP templates completely.⁵ It should be noted that a very thin layer of fibers is preferable for the thermal annealing process, as otherwise the fibers will be partially fused together to form bundles after annealing.

Fabrication of Er-Doped SiO₂ Nanofibers. In a typical experiment for the preparation of 4.1 at. % Er-doped SiO₂ nanofibers, 0.12 g of Er(III) isopropoxide and 1.8 g of tetraethyl orthosilicate (TEOS, 98%, Aldrich Chemical Co.) were dissolved in a mixture of 1.0 mL of ethanol and 1.0

mL of acetic acid, which were then mixed well with 0.61 g of PVP in 2.5 mL of ethanol. The remaining experimental conditions are the same as those used for the preparation of Er₂O₃ nanofibers.

Fabrication of Er-Doped GeO₂ Nanofibers. In a typical experiment for the preparation of 2.0 at. % Er-doped GeO₂ nanofibers, 0.02 g of Er(III) isopropoxide and 0.81 g of tetraethoxygermane (Gelest, Inc.) were dissolved in a mixture of 1.0 mL of methanol (AAPER Alcohol and Chemical Co.) and 0.5 mL of acetic acid, which was further mixed well with 0.30 g of PVP in 1.2 mL of methanol. This mixture was then used to prepare electrospun nanofibers using a 20 kV accelerating voltage. The other experimental conditions are the same as those used for the preparation of Er₂O₃ nanofibers.

Fabrication of Crystalline Er-Doped GeO₂ NWs by a VLS Process. Similar to Er-doped Ge NWs,^{3b} a two-step process was used to fabricate crystalline Er-doped GeO₂ NWs. First, using fabrication methods described previously, crystalline GeO₂ NWs were prepared via a VLS synthetic route that was assisted by a carbothermal reduction reaction to provide the vapor source. In this system, quartz tubing with a 20 mm inner diameter (i.d.) was used as the reactor that was sealed at one end and contains a small hole (with the width of an 18 gauge needle) at the other. In a typical reaction, an alumina boat containing a mixture of 0.0470 g of carbon (J. T. Baker) and 0.1989 g of GeO₂ powder (99.999%, Alfa Inorganics, Inc.) in a C:Ge molar ratio of 2:1 was placed in the reactor. A 5 × 15 mm p-type Si wafer piece deposited with sputtered Au islands was attached vertically to the side of another alumina boat that was positioned in the quartz tube reactor ~2 cm from the edge of the oven. The boat containing a mixture of carbon and GeO₂ was heated by a 30 cm ceramic oven at 940 °C for 15

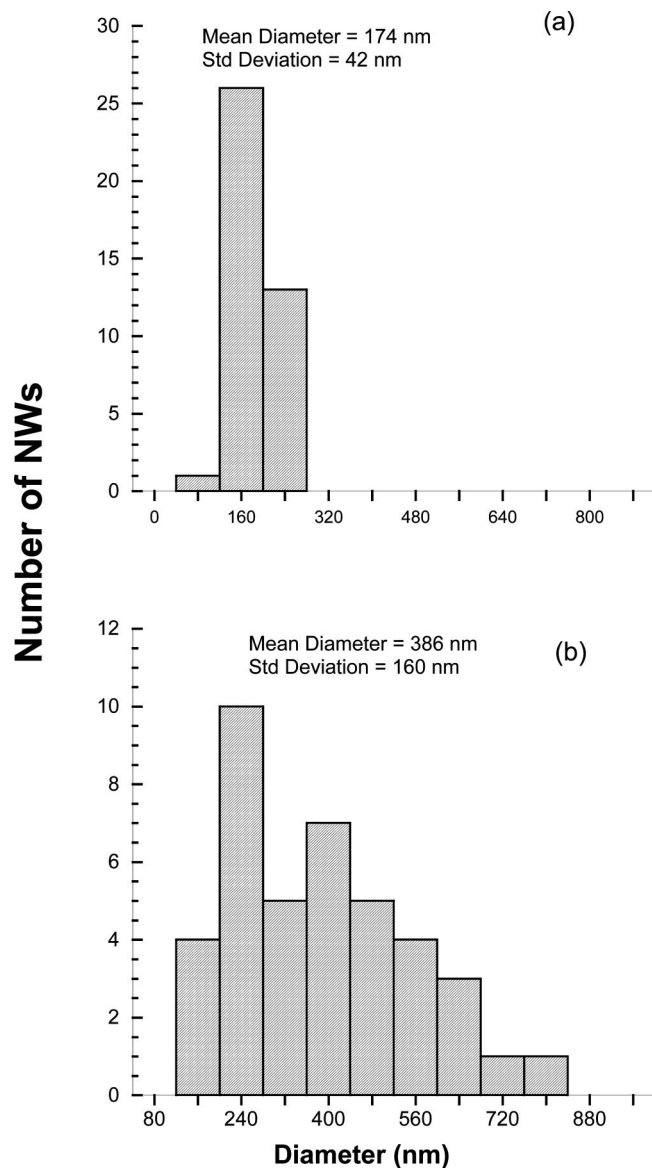


Figure 4. Diameter distributions of (a) a 2% Er-doped SiO₂ nanofiber sample annealed at 500 °C in air for 3 h and (b) as-formed 2% Er-doped SiO₂/PVP nanofibers.

min. The growth temperature of the GeO₂ NWs is ~563 °C, close to that of the above-mentioned Ge NWs. It should be stressed that the optimal nanowire coverage is achieved with the use of the vertical positioning of the Si substrate due presumably to the presence of a critical germanium oxide vapor concentration at that location. At the end of the reaction period, thick films can be easily seen on the Si wafer. In the second step, Er³⁺ ions were deposited on GeO₂ NWs using a chemical vapor deposition (CVD) method similar to that reported previously for producing Ge NWs containing surface-enriched Er³⁺ ions.^{3b} In brief, the precursor Er(tmhd)₃ was heated to 145 °C in a bubbler, and Er(tmhd)₃ vapor was transported downstream by helium (Praxair, UHP grade at a flow rate of 3000 sccm) to a pyrolysis oven operating at 500 °C where the as-prepared sample is located. The as-formed Er-doped GeO₂ NWs were annealed at 600 °C in air for 1 h to obtain near-IR photoluminescence.

Instrumentation. Structural characterization of nanofiber samples was performed using both scanning and transmission

electron microscopies. A JEOL JSM-6100 SEM equipped with a EDX analysis system operating at 20 kV was used to record SEM images and perform elemental analyses of macroscopic nanofiber samples. A Philips EM300 operating at 60 kV was also used to take TEM measurements. Specimens for TEM characterization were prepared by dispersing the sample with a 10 μL drop of 2-propanol and then placing the drop onto a copper grid.

A Hummer VII sputtering system (Anatech, Ltd.) was used to deposit the necessary gold catalyst films for the VLS process. Infrared spectra were collected using a MIDAC M4000 FT-IR spectrometer with a resolution of 4 cm⁻¹. X-ray diffraction (XRD) patterns were collected using a PW Philips diffractometer operating at 35 kV and 30 mA. Copper Kα irradiation with a wavelength of 1.540 56 Å was used as an X-ray source. The angle 2θ (θ = Bragg diffraction angle) ranges from 20° to 110° with a step rate of 0.02° per 3 s for each measurement. Near-IR photoluminescence (PL) spectra were obtained using an Applied Detector Corp. liquid N₂-cooled Ge detector in conjunction with a Stanford Research Systems chopper/locked-in amplifier and an Acton Research Corp. 0.25 m monochromator. Excitation was provided by a Coherent Ar⁺ Innova 300 laser. Emitted light was collected at a 40° angle relative to the excitation direction. A 1000 nm cutoff filter (Melles Griot) was positioned over the monochromator entrance slit to filter out second- and third-order light.

Results and Discussion

Er₂O₃ Nanofibers. Figure 1 presents SEM images of as-formed Er₂O₃/PVP fibers and the fibers annealed at 500 and 700 °C in air for 3 h. It can be easily seen that the as-formed nanofibers are smooth and uniform in terms of width (Figure 1a). In order to obtain pure inorganic fibers, a high-temperature anneal is employed to remove the organic PVP templates. It was found that the structure of the nanofibers was maintained after being annealed at 500 °C in air for 3 h (Figure 1b). After being annealed at 700 °C in air for 3 h, however, the nanofibers were partially deformed with some interfiber connections formed as shown in Figure 1c. Figure 1d shows the corresponding EDX spectrum of an associated Er₂O₃ nanofiber sample. The spectrum suggests that this sample is composed solely of erbium oxide, since the presence of a Be window in the EDX system precludes oxygen detection in this configuration. As it is necessary to coat a 10 nm Au layer on the sample to obtain clearer SEM images, a corresponding Au peak in the EDX spectrum is observed.

Figure 2 shows the diameter distributions of as-formed Er₂O₃/PVP nanofibers and the nanofibers annealed at 500 °C in air for 3 h. The average diameter of the nanofibers has been reduced from 345 to 180 nm (by 48%) due to removal of the PVP templates.⁵

Er-Doped SiO₂ Nanofibers. Figure 3a shows the SEM image of as-prepared Er-doped SiO₂/PVP fibers, with structures observed in the width range of hundreds of nanometers. Figure 3b is the SEM image of Er-doped SiO₂ nanofibers annealed at 800 °C for 3 h. The diameters of these

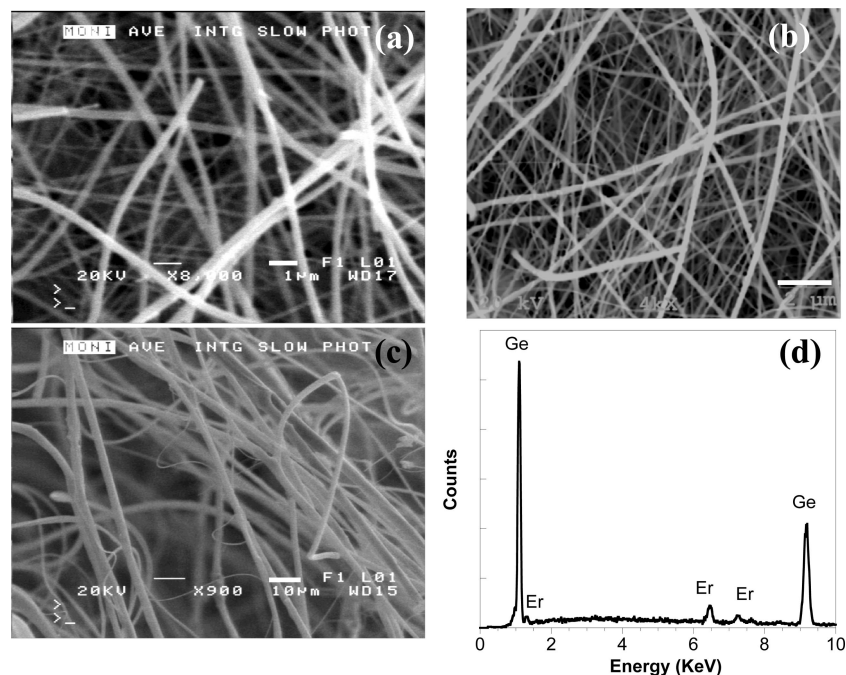


Figure 5. SEM images of (a) as-prepared Er-doped GeO_2/PVP fibers using methanol as a solvent; fibers were prepared with an erbium concentration of 4%. (b) Fibers annealed at 500 °C for 3 h in air. (c) As-prepared Er-doped GeO_2/PVP fibers using ethanol as solvent. (d) EDX spectrum of ~4% Er-doped GeO_2 nanofibers. Scale bar for (a) is 1 μm , (b) is 2 μm , and (c) is 10 μm .

annealed fibers have been greatly reduced, due likely to the removal of the organic PVP templates and accompanying structural rearrangement of the silica matrix. Figure 3c is a typical TEM image of an Er-doped SiO_2 nanofiber sample annealed at 700 °C in air for 3 h, reflecting a nanofiber diameter of about 73 nm. The EDX spectrum of Er-doped SiO_2 nanofibers (Figure 3d) prepared with an erbium concentration of 2% confirms the presence of both erbium and silicon with an atomic ratio of ~1:50. A 10 nm Au layer was also coated on this sample to obtain clearer SEM images, which is again reflected in its EDX spectrum.

Figure 4 shows the diameter distributions of a 2 at. % Er-doped SiO_2 nanofiber sample and a sample annealed at 700 °C in air for 3 h. The average diameter has been reduced by 55% after the 700 °C anneal. In these experiments, Er-doped SiO_2 nanofibers with various concentrations of Er^{3+} ions can be simply prepared by adding different amounts of erbium precursor in a given amount of TEOS solution. In general, the concentration of erbium ions does not affect the general morphology of the fibers in terms of diameter due to its relatively low concentration.

Er-Doped GeO_2 Nanofibers. Characterization. Figure 5a shows a SEM image of as-prepared Er-doped GeO_2/PVP fibers at an erbium concentration of 4 at. %. The surface morphology of the as-prepared fibers are relatively smooth with a average diameter of ~618 nm. Figure 5b is the SEM image of the fibers annealed at 500 °C for 3 h in air. While the surface morphology remains relatively smooth, after annealing the fibers take on a grayish color, in contrast to the whitish appearance of Er_2O_3 nanofibers. This grayish color is presumably caused by the presence of residual GeO_x that was formed by the carbothermal reducing reaction between the carbon (produced after the

decomposition of PVP polymer) and the germanium(IV) precursor.¹¹

To fabricate Er-doped GeO_2 fibers of the target nanoscale width, the reactivity of the Ge(IV) butoxide precursor, and higher viscosity of ethanol must be taken into account. If ethanol instead of methanol is used as the solvent, the solution will be too viscous to be suitable for electrospinning, and fibers of micron size in diameter are obtained (as shown in Figure 5c). Viscosity is a critical factor that can greatly affect the morphology of electrospun nanofibers,⁵ and methanol is much less viscous than ethanol (0.59 mPa·s vs 1.2 mPa·s at 20°).¹² An EDX spectrum (Figure 5d) confirms that there is ~4% erbium in the GeO_2 nanofibers, where Ge-L α and Er-L α peaks lie at 1.2 and 6.9 keV, respectively.

The diameter distributions of as-formed 2 at. % Er-doped GeO_2 nanofibers and those annealed are shown in Figure 6. The average diameter was reduced from 618 to 388 nm after a 500 °C annealing in air for 3 h, which corresponds to a 37% reduction in diameter.

Effect of Annealing Temperatures on Er-Doped GeO_2 Fiber Morphology. As pointed out above, Er-doped GeO_2 fibers annealed at various temperatures have quite different colors and morphologies. The fibers annealed at 500 and 700 °C are dark and light grayish, respectively. However, the color of the fibers annealed at 900 °C is white. It is known that GeO has a dark color and sublimates at 710 °C.¹³ It is possible that some GeO_x formed by the carbothermal reducing reaction during annealing process might be

- (11) Wu, X. C.; Song, W. H.; Zhao, B.; Sun, Y. P.; Du, J. J. *Chem. Phys. Lett.* **2001**, *349*, 210.
- (12) Haidekker, M. A.; Brady, T. P.; Lichlyter, D.; Theodorakis, E. A. *Bioorg. Chem.* **2005**, *33*, 415.
- (13) Hu, J. Q.; Li, Q.; Meng, X. M.; Lee, C. S.; Lee, S. T. *Adv. Mater.* **2002**, *14*, 1396.

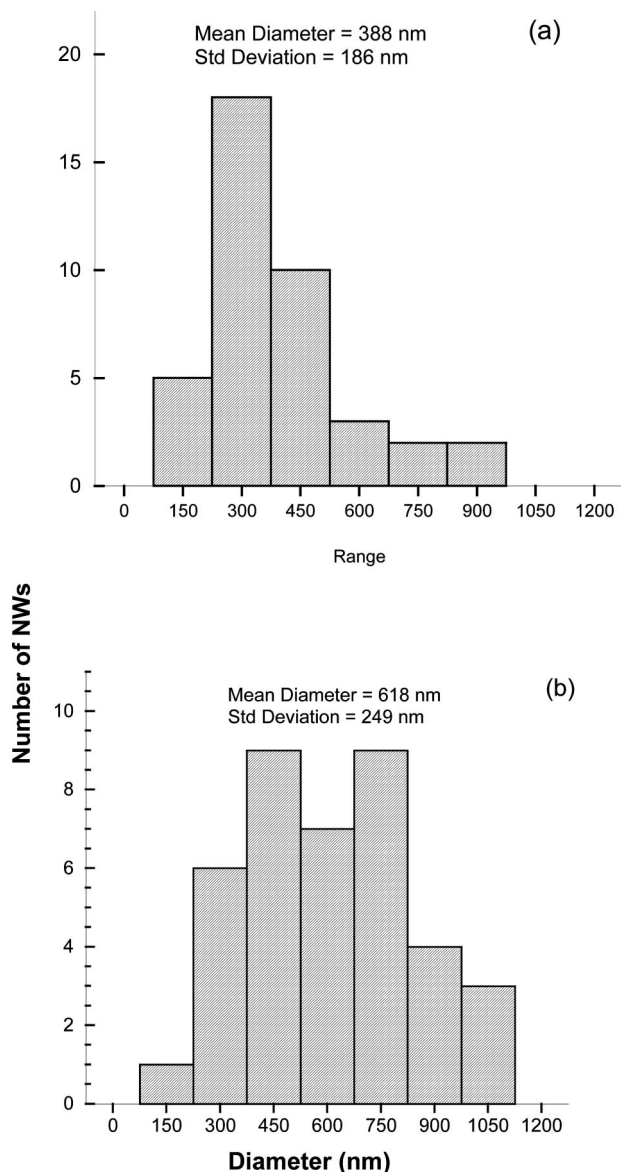


Figure 6. Diameter distributions of (a) 2% Er-doped GeO₂/PVP nanofibers annealed at 500 °C in air for 3 h and (b) as-formed 2% Er-doped GeO₂/PVP nanofibers.

trapped in the host materials when the temperature is lower than the sublimation point of GeO. As a consequence, the fibers annealed at 500 and 700 °C appear quite dark. When the annealing temperature is above the sublimation point of GeO, GeO_x becomes more volatile such that much less GeO_x could be trapped in the fiber and only white GeO₂ is left. It is also possible that GeO_x tends to be completely oxidized into GeO₂ at higher temperatures so that the fibers appear whitish in terms of appearance.

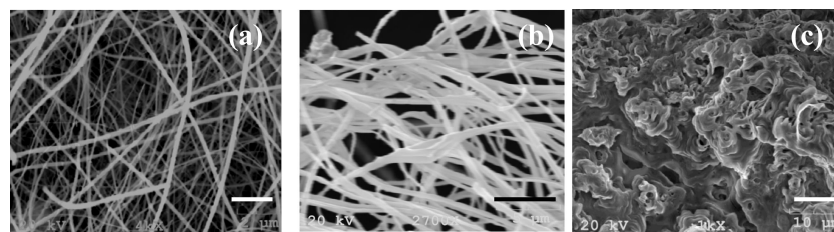


Figure 7. SEM images of Er-doped GeO₂ nanofibers annealed at (a) 500, (b) 700, and (c) 900 °C in air for 3 h. Scale bar for (a) is 2 μm, (b) is 5 μm, and (c) is 10 μm.

It was also found that the morphologies of Er-doped GeO₂ nanofibers changed drastically with increasing annealing temperature. Figure 7 shows SEM images of Er-doped GeO₂ nanofibers annealed at 500, 700, and 900 °C for 3 h in air. The fibers can maintain their morphology after being annealed at 500 °C and start to grow thicker when they were annealed at 700 °C. The formation of thick nanofibers is probably due to an Oswald ripening effect; that is, small islands grow into larger islands due to the chemical potential differences between islands.¹⁴ The fibers were totally fused together, and no individual fibers can be observed after being annealed at 900 °C. The presence of impurities such as erbium ions might result in the decrease of the melting point of GeO₂, which leads to the fusion of the fibers at the temperature below the melting point of GeO₂ (1115 °C). Another feasible possibility is that there is a feature size-dependent reduction in melting point that may influence this change in morphology with heating.¹⁵

FT Infrared (IR) Vibrational Spectroscopy of Er-Doped GeO₂ Nanofibers. FT-IR spectra of Er-doped GeO₂ nanofibers annealed at various temperatures are shown in Figure 8. All spectra have a weak peak at ~432 cm⁻¹ in the low-frequency region, which is attributed to trace amounts of the rutile phase GeO₂.¹⁶ The absence of a C=O stretching vibration at 1660 cm⁻¹ means that the PVP polymer has been completely removed by this thermal annealing process.¹⁷ The FT-IR spectrum of the fiber sample annealed at 900 °C matches well that of standard quartz phase GeO₂,¹⁶ which suggests that this sample has been completely oxidized. Three peaks at 517, 550, and 586 cm⁻¹ are from the O-Ge-O bending vibrations, and another two peaks at 872 and 962 cm⁻¹ are from the asymmetric and symmetric O-Ge-O stretching vibrations, respectively.¹⁸ For the Er-doped GeO₂ fibers annealed at 500 and 700 °C, their FT-IR spectra only show two broad peaks in the ranges of 550–650 and 800–950 cm⁻¹, which indicates that they might be composed of amorphous GeO₂ or GeO_x.¹⁹

Er-Doped Crystalline GeO₂ NWs. Figure 9a shows the SEM image of as-prepared GeO₂ nanowires prepared through a vapor transport method combined with a carbothermal reduction reaction. A Si wafer coated with an 8 nm thick sputtered Au film was used as substrate, and the reaction time was 30 min. These GeO₂ nanowires have diameters ranging from 1 to 8 μm and lengths up to hundreds of microns. Figure 9b is the SEM image of the GeO₂ NWs prepared using a more brief 15 min reaction time. The typical diameter of these nanowires is reduced to ~120 nm, while their typical lengths are shortened to

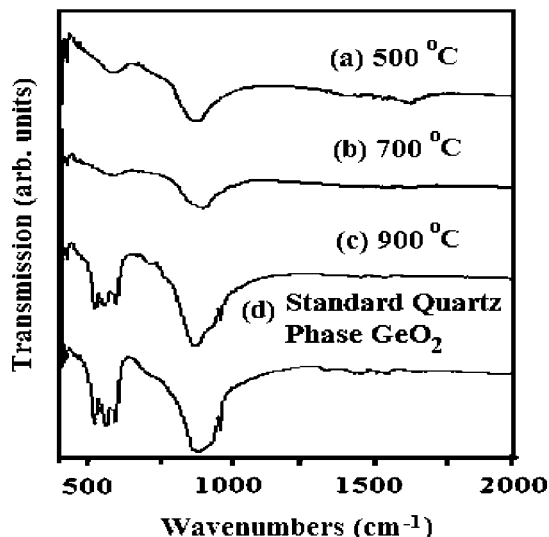


Figure 8. FT-IR spectra of Er-doped GeO₂ nanofibers annealed in air for 3 h at (a) 500, (b) 700, and (c) 900 °C and (d) standard quartz phase GeO₂.

the tens of microns range. In general, shorter reaction times lead to the formation of thinner and shorter GeO₂ nanowires. Figure 9c shows the SEM image of GeO₂ NWs produced on the middle part of the Si wafer. These NWs are much thicker than those produced on the back area of the Si wafer due to the existence of an intrinsic temperature gradient in the reactor. The front part is hotter than the back part because of the former's proximity to the ceramic oven. Therefore, the gold catalysts on the front part of the wafer can grow larger, resulting in the formation of thicker NWs in accordance with the VLS mechanism. These thicker NWs (Figure 9c) have diameters and lengths range from 1 to 2 μm and 10 to 20 μm, respectively. A TEM image of a typical GeO₂ nanowire

is shown in Figure 9d. The nanowire has a diameter of ~62 nm, and the presence of a catalyst on the tip of the NW implies that the NW was grown via a VLS synthetic route.

A XRD pattern of as-formed GeO₂ nanowires is shown in Figure 10. All diffraction peaks match well those of the standard hexagonal germanium dioxide except for the peak at 2θ of 69.1°, which is from the Si (100) wafer (ICDD PDF # 36-1463, GeO₂; ICDD PDF # 27-1402, Si). The sharp diffraction peaks indicate that these nanowires are highly crystalline. The diffraction intensity ratio of (101) to (102) for this sample is about 11:1; this is much higher than the 5:1 ratio for the standard hexagonal GeO₂, which suggests that the GeO₂ NWs might have a preferred (101) growth direction.²⁰

Figure 11a shows the SEM image of Er-doped GeO₂ NWs prepared by exposure of GeO₂ NWs to erbium vapor for 1 h. The diameters of the NWs are very close to those of the GeO₂ NWs due to the thin coating of erbium. The corresponding EDX spectrum (Figure 11b) suggests that the erbium concentration is about 8.5 at. %, which is similar to that of the Er-doped Ge NWs reported previously.^{3b}

Near-IR Photoluminescence. The near-IR photoluminescence properties of these three types of nanofibers, along with that of erbium-doped SnO₂,²¹ containing different erbium concentrations and under various annealing conditions were systematically investigated. Furthermore, the PL excitation spectrum of Er-doped GeO₂ NWs prepared via a VLS synthetic route is compared with those of Er-doped Ge NWs and GeO₂ nanofibers that were prepared through the combined sol-gel/electrospinning approach; this is done in order to investigate similarities and differences in structure and composition.

Figure 12 shows a comparison of the PL spectra of nanofiber samples of Er₂O₃, Er-doped SiO₂, GeO₂, and SnO₂.

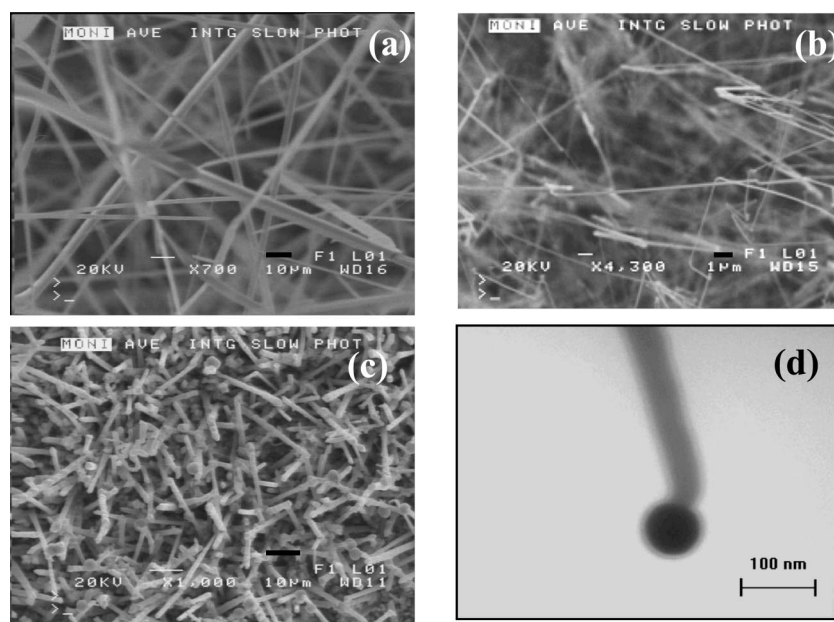


Figure 9. SEM images of (a) GeO₂ NWs grown using a 30 min reaction time, (b) GeO₂ NWs grown using a 15 min reaction time, and (c) the most front part of the sample prepared using a 30 min reaction time. (d) TEM image of a typical GeO₂ NW with a catalyst on its tip (dark contrast). Note: all GeO₂ NWs were prepared at 940 °C on Si containing 8 nm Au catalyst islands. Scale bar for (a) is 10 μm, (b) is 1 μm, and (c) is 10 μm.

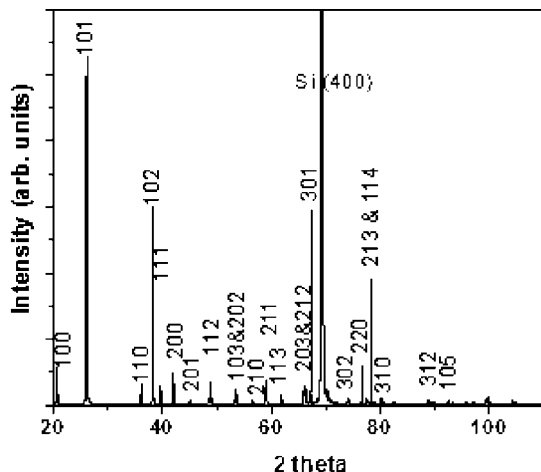


Figure 10. X-ray diffraction (XRD) pattern of as-formed GeO₂ NWs prepared using a 15 min reaction time. The diffraction peak at 69.1° is from the single crystal Si (100) wafer.

It is important to emphasize that all Er-doped nanofibers described in this figure were annealed at 700 °C, except for Er₂O₃ fibers, which were annealed at 500 °C. (Recall that Er₂O₃ nanofibers are partially fused together at the higher annealing temperature of 700 °C.) These temperature values are selected because they are high enough to completely remove the organic template but below a value where the fibers fuse together—hence, the 1-D fiber morphology is retained. It should be noted that all as-formed nanofibers are not emissive unless they have been annealed at high temperatures. This is due to the presence of organic PVP fibers that could quench the PL through the resonant energy transfer from excited Er³⁺ ions to C–H vibrations.^{22,23} High-temperature annealing can also help diffuse the erbium ions uniformly into the host oxide matrix so that Er–Er clustering interactions (also a source of quenching) are relieved.²⁴ Another source of PL quenching in Er³⁺-containing materials is OH moieties,^{25,26} through either physisorbed water or hydroxyl groups covalently present. To probe this influence, the infrared vibrational spectra of a series of Er-doped GeO₂ nanofibers in the OH stretching region (3000–4000 cm⁻¹) were recorded as a function of annealing temperature (500, 700, and 900 °C) (Figure 13a). It confirms that the content of OH groups decreases as anneal temperature increases. However, in the case of a 2 mol % Er-doped GeO₂ nanofiber

sample, the PL intensity of the fibers annealed at 500 °C in air is higher than that at 700 °C, probably due to the loss of GeO_x sensitizer at a relatively higher temperature (Figure 13b); this effect presumably dominates any contribution by hydroxyl groups for the lower temperature-annealed samples. After being annealed at 900 °C, all fibers were fused together and condensed into relatively thick spheres, which makes a quantitative PL comparison difficult.

Among these four types of nanofibers, Er₂O₃ nanofibers emit the weakest luminescence at 1.54 μm due to the high concentration of erbium ions present in this type of fiber. High erbium concentrations can also cause serious up-conversion and excited-state absorption effects, resulting in the decrease of the PL intensity.^{22,27} Furthermore, erbium ions in crystalline Er₂O₃ ideally have an octahedral coordination environment, in which the 4f–4f transitions are forbidden, resulting in weak Er-related emission. For this series of samples, Er-doped SiO₂ and SnO₂ nanofibers both can emit luminescence at 1540 nm with an intensity intermediate between that of erbium oxide and germanium oxide hosts. However, the PL intensity of Er-doped SiO₂ fibers is stronger than that of Er-doped SnO₂ fibers when both fibers are annealed at 700 °C. Er-doped GeO₂ fibers emit the strongest luminescence at 1.54 μm among these four types, which is about an order of magnitude stronger than that of Er-doped SiO₂ nanofibers. This strong increase in PL intensity, along with a different emission mechanism, is likely related to the presence of GeO_x, which will be discussed in detail later.

Figure 14a shows the PL spectra of the Er-doped SiO₂ nanofibers with erbium concentrations ranging from 1 to 4%. When the erbium concentration is increased from 1 to 2%, the PL intensity is enhanced by almost 4 times due to the presence of increased amount of optically active Er³⁺ ions. However, the PL intensity of Er-doped SiO₂ fibers with a 4% erbium concentration is still only 10% higher than that of the fibers with a 2% Er concentration. This phenomenon is probably related to the relatively lower solubility of Er³⁺ ions in the silica host. At higher erbium concentrations, a certain amount of Er³⁺ ions will precipitate from the host matrix and become optically inactive.^{27,28} As a consequence, the PL intensity does not increase linearly when the erbium concentration is increased.

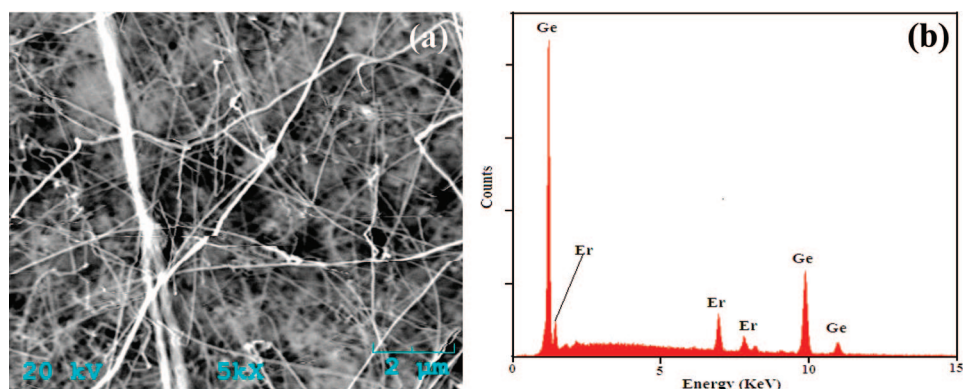


Figure 11. (a) SEM image of Er-doped GeO₂ NWs that were exposed to erbium vapor for 1 h; scale bar shown is 2 μm. (b) Associated EDX spectrum of the sample.

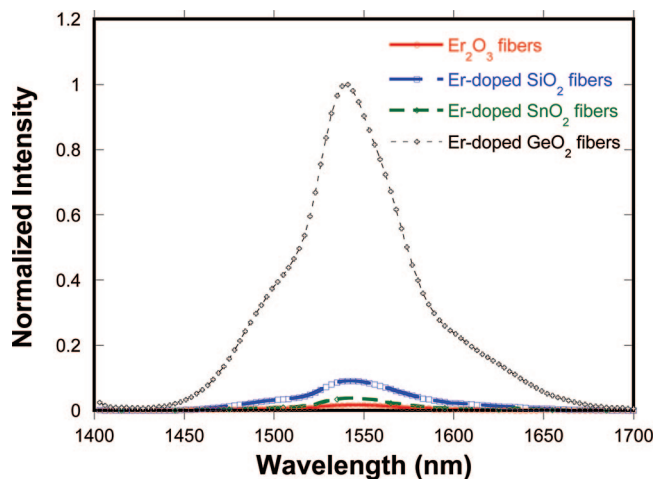


Figure 12. PL spectral comparison of all four types of nanofibers (a) Er_2O_3 , (b) Er-doped SnO_2 , (c) Er-doped SiO_2 , and (d) Er-doped GeO_2 . Note: all Er-doped nanofibers were annealed at 700°C except for Er_2O_3 nanofibers, which were annealed at 500°C .

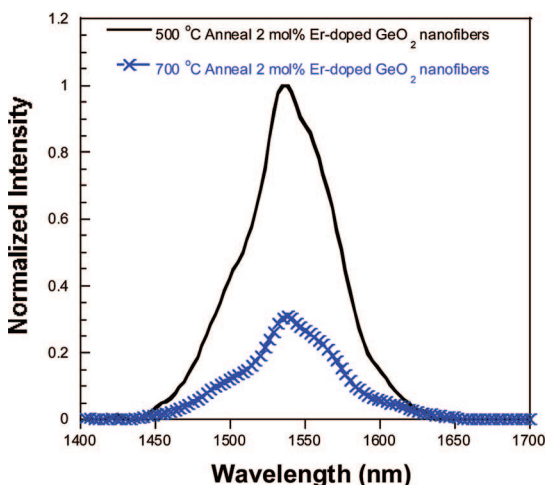
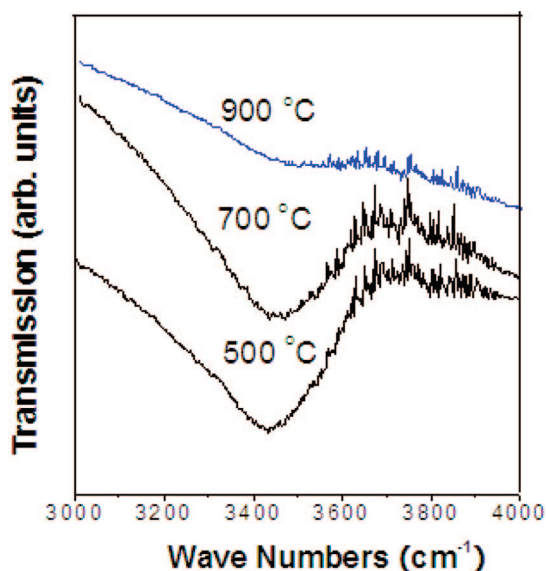


Figure 13. (a) FT IR spectra of Er-doped SiO_2 nanofibers in the $3000\text{--}4000\text{ cm}^{-1}$ region annealed at 500 , 700 , and 900°C in air for 3 h. (b) Corresponding PL spectra of Er-doped GeO_2 nanofibers annealed at 500 or 700°C in air for 3 h.

Figure 14b shows the PL spectra of Er-doped GeO_2 nanofibers with erbium concentrations ranging from 0.5 to 2 at

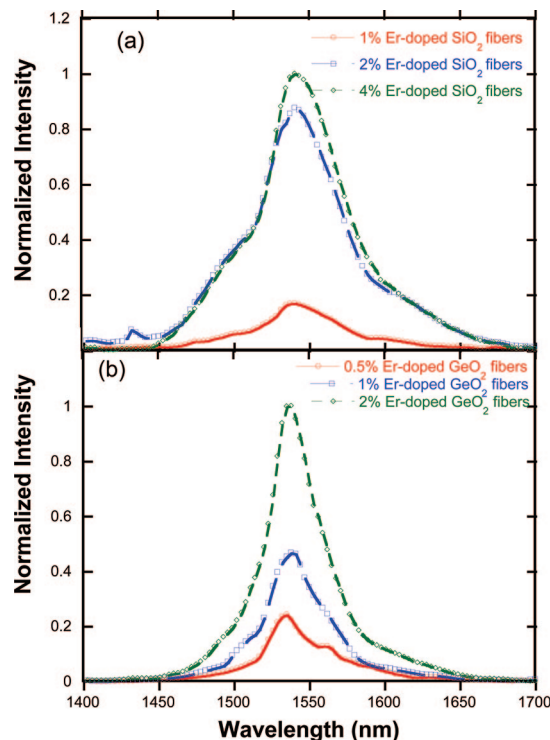


Figure 14. (a) PL spectra of Er-doped SiO_2 nanofibers with erbium concentrations ranging from 1 to 4% (atomic percentage). Note: all fibers were annealed at 700°C in air for 3 h. (b) PL spectra of Er-doped GeO_2 nanofibers with erbium concentrations ranging from 0.5 to 2 at. %. Note: all fibers were annealed at 500°C in air for 3 h.

2 at. %. It is found that the PL intensity is increased in a nearly linear fashion with increasing erbium concentration, which also suggests that there is no significant precipitation of erbium ions in this concentration range. The relatively sharp line width associated with this peak infers that erbium ions are located in a relatively homogeneous coordination environment.²⁹

PL excitation spectra were also employed to further investigate the mechanism of erbium luminescence in these fibers (Figure 15a). In the cases of Er_2O_3 , Er-doped SnO_2 , and SiO_2 nanofibers, the 488 and 514 nm laser excitation lines provide the strongest emission intensity for a given sample, reflecting a direct excitation pathway of the erbium ions in these nanofibers.^{2,3} For such a mechanism, the use of 488 nm (or 514 nm) excitation wavelength results in promotion to a $^4\text{F}_{7/2}$ (or $^4\text{S}_{3/2}$) level, followed by nonradiative decay to the $^4\text{I}_{13/2}$ level and subsequent emission of the requisite near-IR photon when reaching the $^4\text{I}_{15/2}$ ground state. In stark contrast to the other three types of nanofibers, the PL excitation spectra of Er-doped GeO_2 nanofibers are strongly annealing temperature dependent, as shown in Figure 15b. For the Er-doped GeO_2 nanofibers annealed at 700°C , the PL intensity excited at 476 nm is $\sim 76\%$ of the

- (14) Drucker, J. *Phys. Rev. B* **1993**, *48*, 18203.
- (15) Law, M.; Goldberger, J.; Yang, P. *Annu. Rev. Mater. Res.* **2004**, *34*, 83.
- (16) Madon, M.; Gillet, Ph.; Julien, Ch.; Price, G. D. *Phys. Chem. Miner.* **1991**, *18*, 7.
- (17) Khanna, P. K.; Gokhale, R.; Subbarao, V. V. V. S. *J. Mater. Sci.* **2004**, *39*, 3773.
- (18) Kamitsos, E. I.; Yiannopoulos, Y. D.; Jain, H.; Huang, W. C. *Phys. Rev. B* **1996**, *54*, 9775.
- (19) Zacharias, M.; Bläsing, J. *Phys. Rev. B* **1995**, *52*, 14018.

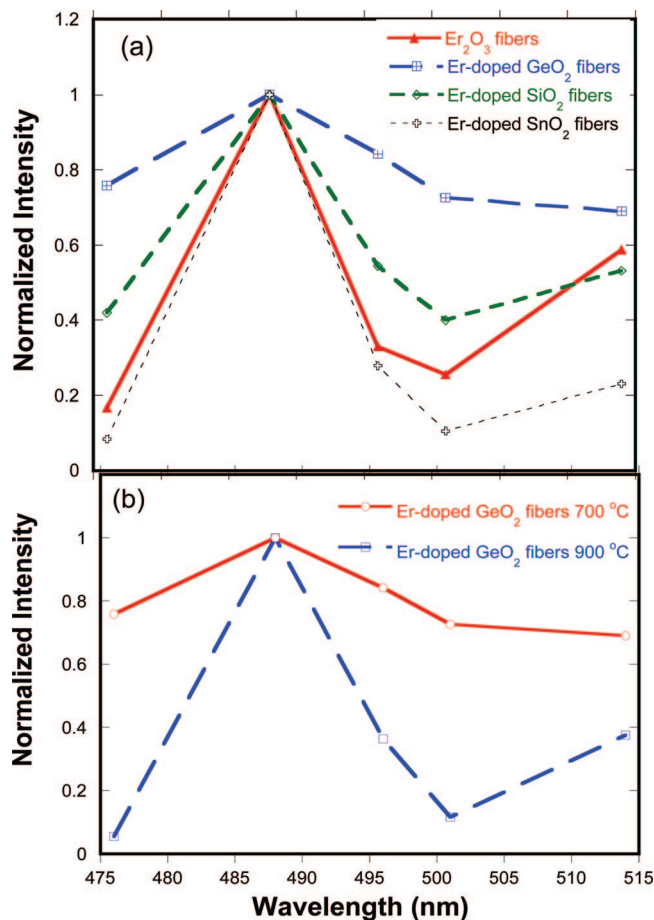


Figure 15. (a) PL excitation spectra of Er₂O₃, Er-doped SnO₂, SiO₂, and GeO₂ nanofibers. (b) PL excitation spectra of Er-doped GeO₂ nanofibers annealed at 700 and 900 °C.

value at 488 nm and stronger than the emission magnitude when excited at 514 nm. This result implies that a carrier-mediated process is responsible for the erbium luminescence in this sample.^{2,3} However, the PL excitation spectrum of the Er-doped GeO₂ nanofibers annealed at 900 °C is quite different from that of the sample annealed at 700 °C, which shows that at higher annealing temperature the 514 and 488 nm laser lines can excite the Er³⁺ ions much more efficiently. The PL intensity excited at 476 nm is only ~5% of the value excited at 488 nm and also much weaker than the emission magnitude when excited at 514 nm. This result suggests that erbium ions in this sample are in a more insulating environ-

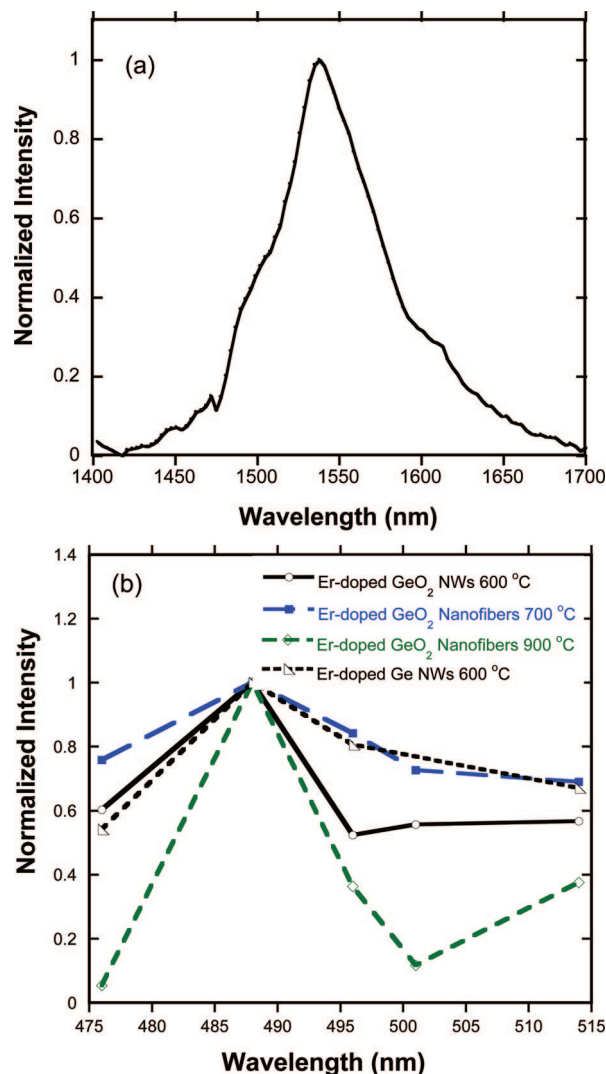


Figure 16. (a) Typical near-IR photoluminescence spectrum of Er-doped GeO₂ nanowires that have been annealed at 600 °C in air for 1 h and exposed to erbium vapor for 1 h. An excitation wavelength of 488 nm was used in this measurement. (b) PL excitation spectra of Er-doped Ge NWs, GeO₂ NWs, and Er-doped GeO₂ nanofibers.

ment and thus only capable of being excited at certain wavelengths correlated to selected ligand field transitions of Er³⁺.

This difference in the PL excitation spectra is presumably caused by the presence of GeO_x. When the nanofibers are annealed at relatively lower temperatures such as 700 °C, some incompletely oxidized GeO_x remains and so are trapped in the nanofiber matrix. This GeO_x can serve as a sensitizer to excite erbium ions via a carrier-mediated process.³ When annealed at higher temperatures such as 900 °C, however, GeO_x could be completely oxidized into GeO₂, resulting in the absence of sensitizers. Therefore, erbium ions can only be directly excited in this sample.

PL Excitation Spectra of Er-Doped Ge NWs, GeO₂ NWs, and GeO₂ Nanofibers. Figure 16a presents a typical near-IR PL spectrum of Er-doped GeO₂ NWs showing strong luminescence at 1540 nm. In Figure 16b, the corresponding PL excitation spectrum of these Er-doped GeO₂ NWs is shown, along with typical profiles for Er-doped Ge NWs and Er-doped GeO₂ nanofibers as well. The Er-doped

- (20) Karim, S.; Toimil-Molares, M. E.; Maurer, F.; Miehe, G.; Ensinger, W.; Liu, J.; Cornelius, T. W.; Neumann, R. *Appl. Phys. A: Mater. Sci. Process.* **2006**, *84*, 403.
- (21) Wu, J.; Coffey, J. *J. Phys. Chem C* **2007**, *111*, 16088–16091.
- (22) Polman, A.; van Veggel, F. *J. Opt. Soc. Am. B* **2004**, *21*, 871.
- (23) Quochi, F.; Orru, R.; Cordella, F.; Mura, A.; Bongiovanni, G.; Artizzu, F.; Deplano, P.; Mercuri, M. L.; Pilia, L.; Serpe, A. *J. Appl. Phys.* **2006**, *99*, 053520.
- (24) Serna, R.; Snoeks, E.; van den Hoven, G. N.; Polman, A. *J. Appl. Phys.* **1994**, *75*, 2644.
- (25) Hui, Y. Y.; Shih, P.-H.; Sun, K.-J.; Lin, C.-F. *Thin Solid Films* **2007**, *515*, 6754.
- (26) Feng, X.; Tanabe, S.; Hanada, T. *J. Non-Cryst. Solids* **2001**, *281*, 48.
- (27) Snoeks, E.; Kik, P. G.; Polman, A. *Opt. Mater.* **1996**, *5*, 159.
- (28) Snoeks, E.; van den Hoven, G. N.; Polman, A. *IEEE J. Quantum Electron.* **1996**, *32*, 1680.
- (29) Polman, A.; Jacobson, D. C.; Eaglesham, D. J.; Kistler, R. C.; Poate, J. M. *J. Appl. Phys.* **1991**, *70*, 3778.

Ge and GeO₂ NWs have been exposed to erbium vapor for 1 h and annealed at 600 °C in air for 1 h, while the 2% Er-doped GeO₂ nanofibers have been annealed at 700 or 900 °C in air for 3 h. It can be seen that the PL excitation spectra of Er-doped Ge NWs, GeO₂ NWs, and GeO₂ nanofibers annealed at 700 °C are very similar. They all have a maximum intensity when excited at 488 nm, and the PL intensity excited at 476 nm is very close to that excited at 488 nm. These results suggest that erbium ions in these NWs and nanofibers are excited through a common carrier-mediated process that is assisted by GeO_x. If annealed at the higher temperature of 900 °C, however, the Er-doped GeO₂ nanofibers shift to an excitation profile dominated by intensities excited at 488 and 514 nm, again, a direct excitation pathway.

Summary

In summary, a facile method that combines the advantages of both electrospinning techniques and sol-gel processing has been developed to fabricate Er-doped group IV oxide

nanofibers with various erbium concentrations, diameters, and host identity of group IV elements.

Among all four types of fibers, Er₂O₃ fibers emit the weakest luminescence, and the PL intensity of Er-doped GeO₂ fibers is almost 10 times stronger than that of Er-doped SiO₂ fibers. The PL of Er₂O₃, Er-doped SnO₂, and Er-doped SiO₂ fibers arises from the direct excitation of erbium ions, whereas a carrier-mediated process is the underlying reason for the erbium photoluminescence in Er-doped GeO₂ nanofibers that are annealed at relatively lower annealing temperatures.

For comparison, crystalline Er-doped GeO₂ NWs were prepared via a VLS synthetic route. The PL excitation spectrum of Er-doped GeO₂ NWs is quite similar to those of Er-doped Ge NWs and Er-doped GeO₂ nanofibers annealed at low temperatures, suggesting that the excitation of erbium ions in these types of NWs and nanofibers is assisted by GeO_x through a carrier-mediated process.

Acknowledgment. Financial support by the Robert A. Welch Foundation is gratefully acknowledged.

CM702226X